Effect of external stress on the Fe–Cr phase separation in 15-5 PH and Fe–15Cr–5Ni alloys

Fréderic Danoix, Jacques Lacaze, A. Gibert, Dominique Mangelinck, Khalid Hoummada, Eric Andrieu

Effect of external stress on the Fe–Cr phase separation in 15-5 PH and Fe–15Cr–5Ni alloys

F. Danoix [a,b,c,d,*], J. Lacaze [e], A. Gibert [a,b,c,d], D. Mangelinck [f], K. Hoummada [f], E. Andrieu [e]

[a] Normandie Univ, France
[b] UR, Groupe de Physique des Matériaux - GPM, 76801 Saint Etienne du Rouvray, France
[c] CNRS GPM UMR 6634, 76801 Saint Etienne du Rouvray, France
[d] INSARouen GPM, 76801 Saint Etienne du Rouvray, France
[e] CIRIMAT - Université de Toulouse - ENSIACET, BP 44362, 31030 Toulouse - France
[f] Aix-Marseille Université, CNRS-IM2NP (UMR 7334), Faculté St-Jérôme, Case 261, Av. Escadrille Normandie-Niemen, 13397 Marseille Cedex 20, France

A B S T R A C T

The effect on Fe–Cr phase separation of a uniaxial stress during thermal ageing at 425 °C is investigated on a Fe–15Cr–5Ni steel, a model alloy of commercial 15-5 PH steel. The applied stress is shown to accelerate the ageing kinetics, and influence the morphology of Cr rich domains. A dependence of the phase separation decomposition kinetics on the relative orientations of the load and the crystal local orientation has also been observed.

1. Introduction

15-5 PH is a precipitation hardened (PH) martensitic stainless steel. Semifinished products consist essentially in a workable soft Fe–Cr martensite that is supersaturated in nickel and copper. The high specific properties of this alloy are obtained by means of a final tempering treatment consisting in a slow heating up to 550 °C, holding at that temperature for 4 h, and then air cooling. This treatment leads to the precipitation of finely dispersed nanometric copper particles, which harden the material [1,2]. Significant ductility level is also obtained after this treatment, due to the formation of limited amount of reverted austenite, favored by the relatively high Ni content, and which remains stable at room temperature [2].

Because of its wide range of applications, from mechanical engineering to aircraft industry, this alloy can experience holdings at temperatures up to 400 °C under regular service conditions. In this temperature range, the Fe–Cr solid solution is known to be unstable, and sensitive to the so called '475 °C' embrittlement. The mechanism of embrittlement has been widely studied in binary Fe–Cr alloys in the temperature range 450 to 520 °C [3–5]. Abundant atom probe investigations showed convincingly that the degradation of the material is related to phase separation of the Fe–Cr matrix into an iron rich (α) and a chromium rich (α') phases [6–11]. Depending on the ageing temperature, phase separation can proceed either through a nucleation and growth precipitation process of the α' phase, or through a $\alpha-\alpha'$ Fe–Cr spinodal decomposition. From previous investigations on closely related 17-4, 15-4 and 13-8 PH alloys [12–14], ageing at 450 °C and higher leads to α' precipitation whereas at temperatures lower than 400 °C, embrittlement is due to spinodal decomposition of martensite. The transition temperature between spinodal decomposition and nucleation and growth is thus most likely in this 400–450 °C range for this alloy family. It is also certain that spinodal decomposition is the active phase separation mechanism at lower temperature, such as 300–350 °C, as previously observed in the ferritic phase of duplex stainless steels used for nuclear applications [15].

This Fe–Cr phase separation leads to increased hardness and yield strength together with a significant loss of ductility and a dramatic increase of the ductile-to-brittle transition temperature [16]. This evolution of mechanical properties has been shown to be directly proportional to the advance of the phase separation process [9]. It is therefore of primary importance to characterize in detail this phase transformation mechanism, in particular its temporal evolution, in order to estimate or predict the evolution of the material's mechanical properties, for example when it is to be used as structural parts in aircrafts or nuclear plants.

Among the various possible forming routes for structural parts made out of 15-5 PH, electron beam welding is highly considered. Because of their small thickness and of the high thermal gradient induced by this welding process, weld beads are high stress regions. Very little is currently known regarding the potential influence of high stress on the kinetics of Fe–Cr phase separation, and thus induced evolution of mechanical properties. It is the aim of this study to investigate the Fe–Cr phase separation at intermediate temperature (425 °C) under uniaxial load, and to compare it with the one resulting from standard thermal ageing. For this purpose, a model alloy with composition similar to 15-5 PH, but without Cu, was prepared. As the Cu precipitates were formed

* Corresponding author.
E-mail address: frederic.danoix@univ-rouen.fr (F. Danoix).

Table 1
Atomic compositions of the two investigated alloys. The balance is iron, and standard deviations were measured according to [35].

Alloy	Cr	Ni	Cu	C	N	Si	Mn	Mo
15-5 PH APT	15.8 ± 0.2	4.6 ± 0.1	2.6 ± 0.1	$0.11 < 0.01$	–	0.75 ± 0.02	0.80 ± 0.02	$0.15 < 0.01$
Fe–15Cr–5Ni APT	15.7 ± 0.1	4.91 ± 0.06	–	–	nd*	$0.23 < 0.01$	$0.28 < 0.01$	–
Fe–15Cr–5Ni nominal**	16.0	4.65	–	–	0.05	0.20	0.20	–

* N and Si were not discriminated on mass spectra, and counted as Si.
** Measured by X-ray fluorescence spectrometry.

at 550 °C, they are not thought to experience any significant evolution at these lower temperatures investigated, and thus not influence significantly the evolution of the mechanical properties of the martensitic matrix. To confirm this assumption, a comparison between 15-5 PH and model Cu free alloy will be conducted.

2. Experimental

Commercial 15-5 PH alloy, containing 15% Cr, 5% Ni, 4% Cu, 0.04% C (wt%) and small amounts of Si, Mo, Nb and Mn (see Table 1) was purchased from Aubert & Duval company. Its composition corresponds to AFNOR X5CrNiCu15-5. It was produced using the argon oxygen decarburization and electro-slag remelting techniques, and cross rolled down to 15 mm thick plates. The precipitation hardening treatment consists of solutionizing at 1050 °C for 0.5 h, air quenching, followed by a final tempering at 550 °C for 4 h (PH treatment). The model alloy was prepared on demand by Aperam Alloy Imphy, France, using high purity base metals (> 99.995%) vacuum arc melted, hot rolled at 1050 °C, solution treated at 1180 °C for 3 h and air quenched.

For both alloys, 'unaged' refers to the conditions presented in the previous section. Further thermal ageing treatments were conducted in a simple air furnace on both commercial and model alloys. Ageing under external stress is conducted on tensile specimens, loaded with a stress equal to 80 per cent of the yield strength in the unaged conditions in a dedicated furnace. As a consequence, the applied stress is uniaxial along the tensile axis.

Specimens for atom probe analyses were cut from aged plates and tensile specimens after thermo-mechanical treatments. Tensile test specimens were thinned to 0.3 mm in thickness, and cut to 0.3×0.3 mm^2 in cross section using a precision diamond saw. They were about 15 mm long, with their length aligned along the tensile direction. Tips suitable for atom probe tomography analyses were prepared using the standard two stage electrochemical method [17].

Specimens were analyzed with the Ecowatap instrument developed in the University of Rouen, with the following experimental conditions: specimen temperature 80 K, pulse repetition rate 30 kHz, and pulse to standing voltage ratio 19%. Averaged compositions obtained by atom probe analyses are given in Table 1. They are in good agreement with the nominal ones. It should be noted that the chromium concentration in each individual run did not deviate by more than 6% in relative (0.4 at% absolute) from the average value, indicating a good homogeneity of the analyzed materials. Only on some selected runs, few copper rich particles in 15-5 PH alloy, or platelike chromium nitrides in the model alloy were intercepted, making the copper and nitrogen contents fairly different from one run to another. Additional analyses were also conducted on the LEAP 3000HR in the University of Marseille, using the same base temperature and pulse to standing voltage ratio, but with a pulse repetition rate of 200 kHz.

3D reconstructions of atom positions, referred as 3D reconstruction, were generated using both tap3Ddata software for the data collected on the Ecowatap, and IVAS 3.5 for the one collected on the LEAP. Data analyses were all conducted on the tap3Ddata software developed at the University of Rouen.

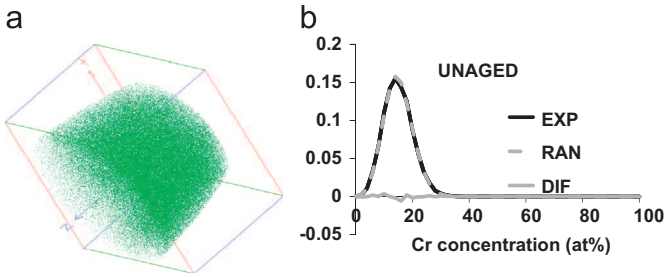

Fig. 1. (a) Distribution of chromium atoms (green) in an unaged specimen of Fe–15Cr–5Ni model alloy. The represented volume is $35 \times 35 \times 25$ nm^3. (b) Chromium concentration frequency distribution analysis corresponding to the same thermal ageing condition (vertical axis is in arbitrary units). (For interpretation of the references to color in this figure legend, the reader is referred to the web version of this article.)

The advance of the Fe–Cr phase separation was measured using the *V* parameter, which is the integral area of the difference (DIF in Figs. 1–5) between the experimental Cr concentration frequency distribution (EXP in Figs. 1–5) of the aged sample and the corresponding binomial distribution with the same average (random solid solution, RAN in Figs. 1–5) [18]. Local concentrations were calculated over volumes containing 50 atoms, which corresponds to about one cubic nanometer [19]. This parameter has been shown to be very sensitive to the extent of phase separation and to vary linearly with the hardness of the material, making it a good parameter for characterizing the evolution of the phase separation process [20]. In this work, the characteristic wavelength of the Fe–Cr phase separation was not used because, as will be shown later, ageing under stress induces a non isotropic evolution of the Fe and Cr rich domains. As a consequence, the measured distance would depend on the direction selected for the measurement, and was not considered as an accurate parameter.

3. Results

3.1. Unaged condition

A first specimen of the Fe–15Cr–5Ni model alloy was analyzed in the unaged condition. As shown in Fig. 1a, the distribution of chromium atoms is homogeneous in the analyzed volume. This is confirmed by the frequency distribution of Cr concentration, shown in Fig. 1b, which is almost identical to the binomial distribution. A χ^2 test was conducted on both distributions, leading to a value of $\chi^2 = 26.1$, with 18 degrees of freedom. Such a value clearly indicates that the hypothesis of a random distribution of Cr atoms cannot be ruled out at the 95% confidence level. The *V* value measured from the difference between experimental and binomial distributions is 0.02, and reported in Table 2. In agreement with previous results [21], such a low value

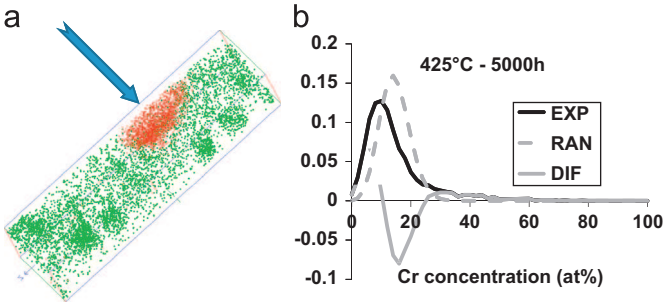

Fig. 2. (a) Distribution of Cr (green) and Cu (red) atoms in 15-5 PH alloy aged at 425 °C for 1000 h. The represented volume is $7 \times 7 \times 30\ nm^3$. (b) Chromium concentration frequency distribution analysis corresponding to the same thermal ageing condition (vertical axis is in arbitrary units). (For interpretation of the references to color in this figure legend, the reader is referred to the web version of this article.)

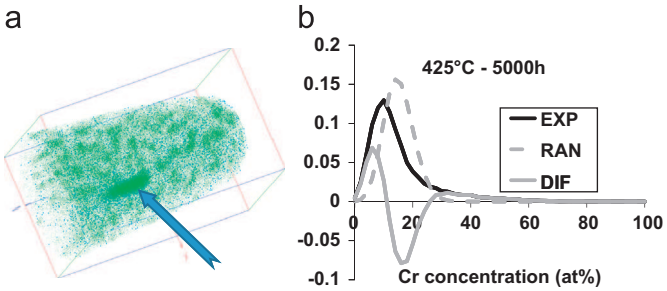

Fig. 3. (a) Distribution of Cr (green) and N (blue) atoms in Fe–15Cr–5Ni model alloy aged at 425 °C for 1000 h. The represented volume is $30 \times 30 \times 50\ nm^3$. (b) Chromium concentration frequency distribution analysis corresponding to the same thermal ageing condition (vertical axis is in arbitrary units). (For interpretation of the references to color in this figure legend, the reader is referred to the web version of this article.)

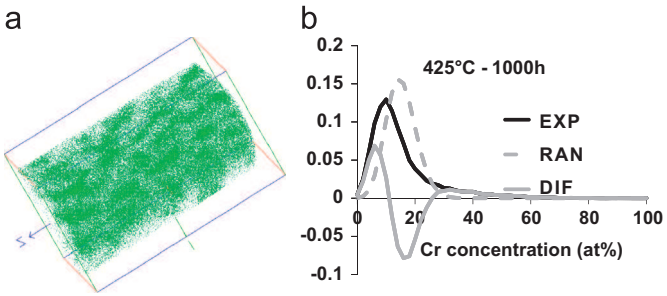

Fig. 4. (a) Distribution of Cr atoms (green) in Fe–15Cr–5Ni model alloy aged at 425 °C for 1000 h under uniaxial load. The represented volume is $20 \times 20 \times 40\ nm^3$. (b) Chromium concentration frequency distribution analysis corresponding to the same thermal ageing condition (vertical axis is in arbitrary units). (For interpretation of the references to color in this figure legend, the reader is referred to the web version of this article.)

indicates that no significant Cr segregation is detected, in agreement with the χ^2 test.

3.2. Thermal ageing at 425 °C

Figs. 2a and 3a show the 3D reconstructions of Cr obtained after ageing at 425 °C for 5000 h, respectively for 15-5 PH and model alloy. Both reconstructions clearly show that Cr fluctuations have developed in the Fe–Cr matrix. The presented reconstructions have been selected to show the additional phases which appear in both materials, namely Cu rich spherical particles and N rich platelets, observed in Figs. 2a and 3a, respectively. The Cu rich particles are the one expected in the commercial 15-5 PH after the precipitation hardening treatment at 550 °C for 4 h,

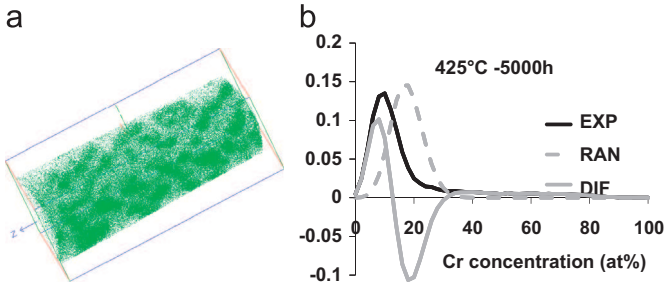

Fig. 5. (a) Distribution of Cr atoms (green) in Fe–15Cr–5Ni model alloy aged at 425 °C for 1000 h under uniaxial load. The represented volume is $23 \times 23 \times 53\ nm^3$. (b) Chromium concentration frequency distribution analysis corresponding to the same thermal ageing condition (vertical axis is in arbitrary units). (For interpretation of the references to color in this figure legend, the reader is referred to the web version of this article.)

Table 2
Measured *V* parameter values for both alloys aged at 425 °C.

Alloy		15-5 PH		Fe–15Cr–5Ni model alloy			
Unaged				0.02			
Thermal ageing	1000 h			0.54	0.52		
	5000 h	0.70	0.71	0.69	0.71		
Uniaxial load ageing	1000 h			0.68	0.64	0.67	0.66
	5000 h			0.77	0.89	1.03	

whereas the N rich platelets correspond to chromium nitrides that formed during ageing at 425 °C in the model alloy. However, these precipitates are observed in only about 1/4 of the analyses, and are definitely not the main microstructural features of specimens thermally aged at 425 °C, which is clearly Fe–Cr phase separation. As the aim of this work is to study the influence of external stress on Cr concentration fluctuations, only the latter were considered for statistical analyses. As a consequence, only volumes at least 10 nm away from the detected particles (i.e. Cu precipitates and chromium nitrides platelets) were used for statistical analysis. For each of the analyzed volumes containing at least 50,000 detected ions, frequency distributions were calculated, and *V* parameters measured. They are reported in Table 2. *V* values obtained after 1000 and 5000 h of ageing are respectively in the ranges 0.52–0.54 and 0.69–0.71. It should be noted that if the volumes containing either Cu particles or CrN platelets would have been included in the statistical analyses, the *V* parameter would not have changed significantly, as it ranges from 0.68 to 0.73 after 5000 h of ageing. No chromium nitride platelet was observed in the model alloy aged 1000 h.

The *V* values reported in Table 2 also indicate that there is only marginal, if any, difference in the advance of the Fe–Cr phase separation between commercial and model alloys, indicating that the considered levels of Cu and N do not affect the kinetics of Fe–Cr phase separation. As a consequence, regarding Fe–Cr phase separation, both alloys can be considered as similar.

3.3. Thermal ageing at 425 °C under uniaxial load.

As both alloys showed the same behavior regarding Fe–Cr phase separation during thermal ageing at 425 °C, it was decided to focus only on the model alloy to investigate the effect of the external stress on the Fe–Cr phase separation. Only model alloy specimen aged at 425 °C for 1000 and 5000 h under uniaxial load were analyzed. Selected 3D reconstructions corresponding to each of these conditions are shown in Figs. 4a and 5a respectively. Both reconstructions clearly show a significant elongation of the Cr rich domains. In the case of one of the specimens aged for

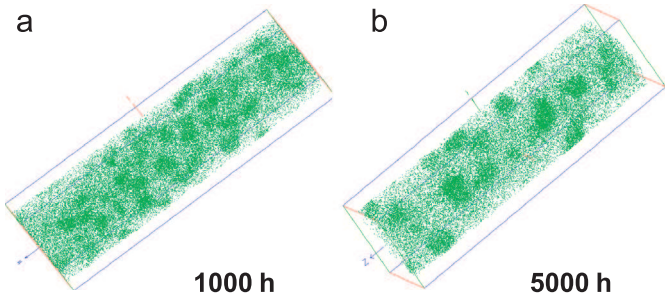

Fig. 6. Distributions of Cr atoms (green) in Fe–15Cr–5Ni model alloy aged at 425 °C under uniaxial load. The represented volumes are $15 \times 15 \times 50\ nm^3$. (For interpretation of the references to color in this figure legend, the reader is referred to the web version of this article.)

1000 h, the elongation is more or less aligned with the specimen axis, i.e. in the load direction, whereas in one of the specimens aged for 5000 h, it appears to be misaligned with respect to the specimen axis with an angle close to 45°. However, as shown in Fig. 6 for both ageing conditions, other analyses showed isotropic Cr rich domains, with no apparent elongation of the Cr rich domains. The elongation of the Cr rich domains is clearly not a systematic effect.

Statistical analyses were also conducted on these specimens, using the same procedure as for thermal ageing. Measured *V* parameter values are reported in Table 2. Conversely to the simple thermal ageing, individual *V* values show a significant scatter, and significantly differ from each other for the various runs.

4. Discussion

4.1. Thermal ageing at 425 °C

The limited scatter of the obtained *V* values for the thermally aged specimens, combined with the very low value obtained on the unaged specimen (see Table 2), confirms that this parameter is an accurate estimate of the advance of Fe–Cr phase separation. The precision of this parameter can be estimated to be about 0.02 units.

The influence of Cu and N on the observed evolution of the investigated alloys can be evaluated on the basis of the presented results. First of all, these elements are responsible for the precipitation of Cu precipitates and CrN nitrides respectively, which have been observed during this study. Based on the number of observed particles and on the overall analyzed volumes, it is estimated that the mean distance between particles (both Cu and CrN) is in the range of 50 to 100 nm. Because of the small total analyzed volume, and therefore poor representativity, these numbers are only rough estimates, and must be considered with care. However, the number density of such particles is very limited, at least two orders of magnitude lower than the one of Cr rich domains, and is not thus believed to affect significantly the present result. This is confirmed when comparing the *V* values obtained when volumes containing such particles are not removed for statistical analyses.

Interestingly, the *V* values measured for the commercial 15-5 PH and model alloy are identical, within the estimated precision of the *V* parameter. The Fe–Cr phase separation process is thus very similar for both alloys. This indicates that neither the Cu precipitation treatment at 550 °C for 4 h, nor the presence of these precipitates in the as received commercial alloy, have any significant effect on the Fe–Cr phase separation mechanism. This is particularly interesting, as it indicates that the Fe–Cr phase separation is not affected by the precipitation hardening treatment at 550 °C, which is only slightly higher than the miscibility gap limit [22]. A consequence of the similar behavior of both alloys with respect to the evolution of the Fe–Cr phase separation is that it is sufficient to study only the model alloy, and that results can be extrapolated confidently to the commercial 15-5 PH alloy. This is the reason why only the model alloy was investigated at 425 °C under uniaxial load.

From the presented literature data, the question of the nature of the transformation mechanism of Fe–Cr phase separation at 425 °C, i.e. spinodal decomposition or nucleation and growth of α′ particles is still open. This information could potentially be derived from the obtained 3D reconstructions. They clearly show that Cr rich domains appear as isolated regions, or particles. It would tend to indicate that the second mechanism is active. However, this morphology is not fully supporting this conclusion, and may be related to another reason. The nominal Cr content of the investigated alloys is 15 at%. The Cr solubility in iron, as measured by atom probe, is 8 at% at 350 °C. According to shape of the miscibility gap, is can be estimated to be approx. 10 at% at 425 °C [23]. Referring to the current analyses, the Cr content in individual Cr rich domains is about 45 to 50 at%. With such concentrations, the volume fraction of Cr rich domains would be lower than 14%, which is significantly lower than the percolation threshold in 3D [24]. Therefore, even if the phase separation mechanism is spinodal decomposition, the developing Cr rich domains would rapidly isolate from each other, and form isolated particles. The present results cannot be used, on their own, to identify the phase separation mechanism, and additional kinetic analyses are necessary to address this point. This result also makes it impossible to study on the basis of the presented results any transition from spinodal decomposition to nucleation and growth (and vice versa) due to the external stress, as predicted by Cahn [25].

4.2. Thermal ageing at 425 °C under uniaxial load.

A major result of the present work is the kinetic evolution of Fe–Cr phase separation during ageing under uniaxial load. As shown in Table 2, *V* values are systematically larger than the one obtained after the same ageing time but without external stress. This evidences a clear accelerating effect of the external stress on the Fe–Cr phase separation. This result is consistent with recent phase field simulations, which showed that an increased local stress field (associated to the presence of dislocations) facilitates, energetically and kinetically, Fe–Cr phase separation [26]. It is also consistent with a very recent work conducted on duplex stainless steels aged at 325 °C [27].

However, an important scatter is observed in the measured *V* values obtained after ageing 5000 h, ranging from 0.77 to 1.03. As shown for the thermally aged specimens, the experimental scatter on *V* measurement was estimated to be 0.02, whereas the difference observed for the specimens aged under external stress is 0.26. The observed scatter in *V* values is a clear indication that significant differences exist between the different analyzed volumes. As such a scatter was not observed in the case of thermally aged specimens, it is unambiguously related to the effect of the external stress. It is therefore concluded that the effect of the applied stress is different from one region of the specimen to the other.

In addition, as shown in Figs. 4a and 5a, an elongation of the Cr rich domains is observed in some analyses. The possibility that this elongation would be due to a reconstruction procedure artifact has first been considered. In that case, the elongation should systematically be either in the analysis direction, or perpendicular to it. The observed disorientation of about 45°

clearly rules out this possibility, and indicates that it is related to a microstructural evolution in the matrix. In addition, the same reconstruction parameters have been used for all specimens, which should lead, in the case of erroneous values, to a systematic elongation in a given direction. The observation of isotropic Cr rich domains in many specimens (see Fig. 6) confirms that reconstruction artifacts cannot be regarded as responsible for the observed elongation of Cr rich domains. The sometime observed elongation is thus a real, but not systematic, nanostructural feature of specimens aged under external stress. This again reveals different local responses of the morphology of the Fe–Cr nanostructure to the applied stress.

The above experimental results show a large disparity in the nanostructure of specimens aged under stress, both in terms of phase separation advance and product morphology. As it was observed to be quite homogeneous in the case of specimens thermally aged, the appearance of certain degree of heterogeneity in the nanostructure must therefore be regarded as an effect of the external stress applied during ageing.

The only possible reason for such a behavior is that the effect of the applied stress is dependent on the local orientation of the crystal with respect to the load direction. Because of the analyzed volume sizes, each atom probe dataset is obtained from one individual grain. Due to the atom probe specimen electrochemical preparation method, grain orientation at the specimen apex cannot be selected prior to analysis, and each individual analyzed grain is randomly oriented with respect to the tip axis. As previously mentioned, the load direction is always parallel to specimen axis, so different randomly selected grain to applied stress orientational configurations have been investigated during this work, and is most likely the reason why significantly different nanostructures have been observed.

The elastic anisotropy, even if very small in the case of Fe–Cr alloys, is enhanced by the external stress. The Cr rich domains will tend to develop along the elastically soft direction of the matrix, i.e. $<100>$ [28], and will thus result in the development of an anisotropic nanostructure. This effect may be similar to the well-known rafting of γ' precipitates in nickel base superalloys. Depending on the orientation of the $<100>$ axis of the grain at the apex of the atom probe specimens, the elongation orientation will not always appear in the same direction in the reconstructed volumes, as observed experimentally.

This orientation argument can also be invoked to explain the observed effect of faster Fe–Cr phase separation under stress. Herny [1] has shown that, even if the kinetic of phase separation is faster under external stress, the hydrostatic stress has no influence on it. This is in accordance with Larché and Cahn's work [29], who predicted that as soon as the process of phase separation is initiated, the hydrostatic component of the stress tensor is much lower than the stress generated by the phase separation itself, and so it is not supposed to modify neither the thermodynamics nor the kinetics of the phase separation. Therefore, deviatoric stress has to be regarded as the source of the acceleration of the phase separation. Even in the case of uniaxial load, the disorientation of the crystal with respect to the load axis will generate deviatoric components in the strain tensor, the strength of which will depend on the respective grain and load axis orientations. It is therefore likely that the local phase separation advance will be dependent on the respective orientation of each grain with the load axis. So, it is most likely that the effect of the external stress on the developed nanostructure (elongation, kinetics) will directly depend upon the orientation of each grain, and result in nanostructural heterogeneities from grain to grain.

Clearly, to predict the local evolution of the Fe–Cr nanostructure during ageing under external stress, a micromechanical model is necessary to evaluate the importance of the deviatoric components, in particular their dependence with the orientation. Such a model could also help to understand the possible effect of the stress level. Indeed, no effect of the external stress was observed in FeCrCoTi alloys aged under 100 MPa stress [30], whereas an obvious effect is observed in our investigations conducted under an external stress of 800 MPa.

From an experimental point of view, studying the correlation between grain and stress disorientation requires the knowledge of the crystal orientation for each analysis. Field ion microscopy inspection of the specimens could provide this information, if conducted prior to atom probe analysis. Unfortunately, it was not conducted in this work. The grain orientation could also be obtained a posteriori from atom probe desorption maps [31] or interstitial atom distribution [32]. Over the presented experimental results, only one desorption map could be successfully used for this purpose. Of course, on the basis of this single result, it was not possible to derive any correlation. On the other hand, it is proposed, for further studies, to use a different approach: atom probe specimen preparation combining electron backscattered diffusion (EBSD) and focused ion beam (FIB) lift out [33]. The absolute orientation of each individual grain can be obtained using EBSD, and, knowing the load direction, the disorientation can be determined for each grain. Site specific lift out [34] could then be conducted from grains showing pertinent disorientations with the load axis, which could be derived from the micro mechanical model.

5. Conclusion

The effect of thermal ageing at 425 °C on phase separation in Fe–15Cr–5Ni alloy has been made, and a comparison has been conducted between ageing without an applied stress and ageing under uniaxial load of 80% of the yield stress. A significant effect of the external stress on the ageing kinetics and morphology of Cr rich formed domains has been observed. A dependence of the respective orientations of the load and the crystal local orientation on the phase separation decomposition kinetics has also been observed. This dependence makes it impossible to study quantitatively the influence of the external stress on the Fe–Cr phase separation from techniques such as hardness measurements, Mossbauer spectrometry or small angle neutron scattering, which integrate the whole grain orientation distribution. It is suggested that a systematic atom probe investigation of the effect of stress on the phase separation in Fe–Cr should be conducted on selected specimens with pre-selected crystal and stress direction orientations, combined with the development of a micromechanical model.

References

[1] E. Herny, PhD Thesis, Institut national polytechnique de Toulouse, Toulouse (France), 2006, (in French).
[2] E. Herny, P. Lours, E. Andrieu, J.M. Cloué, P. Lagain, Evolution of microstructure and impact-strength energy in thermally and thermomechanically aged 15-5 PH, Proceedings of the IMechE 222 (2008) 299–304, J. Materials: Design and Applications.
[3] O.K. Chopra, H.M. Chung, Aging degradation of cast stainless steels: effects on mechanical properties, in: G.J. Theus, J.R. Weeks (Eds.), Proceedings of the 3rd International Symposium on Environmental Degradation of Materials in Nuclear Power Systems—Water Reactor, TMS, Warrendale Pa, 1988, pp. 737–748.
[4] P.H. Pumphrey, K.N. Akhurst, The aging kinetics of CF3 cast stainless steel in the temperature range 300 °C to 400 °C, Materials Science and Technology 6 (1990) 211–219.
[5] H.D. Solomon, L.M. Levinson, Mössbauer effect study of 475 °C embrittlement of duplex and ferritic stainless steels, Acta Metallurgica 26 (1978) 429–442.
[6] S.S. Brenner, M.K. Miller, W.A. Soffa, Spinodal decomposition of iron–32 at% chromium at 470 °C, Scripta Metallurgica 16 (1982) 831–836.

[7] M.K. Miller, J. Bentley, S.S. Brenner, J.A. Spitznagel, Long term thermal aging of type CF8 stainless steel, Journal of Physics (1984) 385–390 45-C9.
[8] T.J. Godfrey, G.D.W. Smith, The atom probe analysis of cast duplex stainless steels, Journal of Physics (1986) 217–222 47-C7.
[9] P. Auger, F. Danoix, A. Menand, S. Bonnet, J. Bourgoin, M. Guttmann, Atom probe and transmission electron microscopy study of aging of cast duplex stainless steels, Materials Science and Technology 6 (1990) 301–313.
[10] M.K. Miller, J.M. Hyde, M.G. Hetherington, G.D.W. Smith, C.M. Elliott, Spinodal decomposition in Fe–Cr alloys: experimental study at the atomic level and comparison with computer models—introduction and methodology, Acta Metallurgica et Materialia 43 (1995) 3385–3401.
[11] S. Novy, C. Pareige, P. Pareige, Atomic scale analysis and phase separation understanding in a thermally aged Fe–20 at% Cr alloy, Journal of Nuclear Materials 384 (2009) 96–102.
[12] M. Murayama, Y. Katayama, K. Hono, Microstructural evolution in a 17-4 PH stainless steel after aging at 400 °C, Metallurgical and Materials Transactions 30A (1999) 345–353.
[13] Z. Guo., W. Sha, D. Vaumousse, Microstructural evolution in a PH13-8 stainless steel after ageing, Acta Materialia 51 (2003) 101–116.
[14] S.D. Erlach, H. Leitner, M. Bischof, H. Clemens, F. Danoix, D. Lemarchand, I. Siller, Comparison of NiAl precipitation in a medium carbon secondary hardening steel and C-free PH13-8 maraging steel, Materials Science and Engineering A 429 (2006) 96–106.
[15] F. Danoix, P. Auger, Atom probe studies of the Fe–Cr system and stainless steels aged at intermediate temperature: a review, Materials Characterization 44 (2000) 177–201.
[16] S. Bonnet, J. Bourgoin, J. Champredonde, D. Guttmann, M. Guttmann, Relationship between evolution of mechanical properties of various cast duplex stainless steel and metallurgical and aging parameters: outline of current EDF programmes, Materials Science and Technology 6 (1990) 221–229.
[17] M.K. Miller, G.D.W. Smith, Atom probe microanalysis: principle and applications in materials science, Materials Research Society, Pittsburg PA, 1989.
[18] D. Blavette, G. Grancher, A. Bostel, Statistical analysis of atom-probe data (I): derivation of some fine scale features from frequency distributions for finely dispersed systems, Journal of Physics (1988) 433–438 49-C6.
[19] J.M. Sarrau, F. Danoix, M. Bouet, B. Deconihout, D. Blavette, A. Menand, The Rouen energy-compensated atom-probe, Applied Surface Science 76 (1994) 367–373.
[20] F. Danoix, P. Auger, D. Blavette, Hardening of aged duplex stainless steels by spinodal decomposition, Microscopy and Microanalysis 10 (2004) 349–354.
[21] C. Lemoine, A. Fnidiki, F. Danoix, M. Hedin, J. Teillet, Mossbauer and atom probe studies on the ferrite decomposition in duplex stainless steels caused by the quenching rate, Journal of Physics: Condensed Matter 11 (1999) 1105–1114.
[22] A. Gibert, Master Degree, University and INSA Rouen (France), 2011, (in French).
[23] J.O. Andersson, B. Sundman, Thermodynamic properties of the Cr–Fe system, Calphad 11 (1987) 83–92.
[24] F. Danoix, PhD Thesis, Univesity of Rouen, 1991, (in French).
[25] J.W. Cahn, Cited in [29].
[26] Y.S. Li, S.X. Li, T.Y. Zhang, Effect of dislocations on spinodal decomposition in Fe–Cr alloys, Journal of Nuclear Materials 395 (2009) 120–130.
[27] J. Zhou, J. Odqvist, M. Thuvander, S. Hertzman, P. Hedström, Concurrent phase separation and clustering in the ferrite phase during low temperature stress aging of duplex stainless steel weldments, Acta Materialia 60 (2012) 5818–5827.
[28] Y. Ustinovshikov, I. Igumnov, V. Koretsky, Decomposition of solid solutions having a tendency toward ordering or separation, Computational Materials Science 21 (2001) 185–196.
[29] F.C. Larché, J.W. Cahn, The interactions of composition and stress in crystalline solids, Acta Metallurgica 33 (1985) 331–357.
[30] S.S. Chou, T.S. Chin, L.C. Yang, Effect of stress-aging on spinodal decomposition and magnetic properties of Fe–Cr–Co–Ti alloys, Scripta Metallurgica 18 (1984) 121–125.
[31] V.J. Araullo-Peters, B. Gault, S.L. Shrestha, L. Yao, M.P. Moody, S.P. Ringer, J.M. Cairney, Atom probe crystallography: atomic-scale 3-D orientation mapping, Scripta Materialia 66 (2012) 907–910.
[32] B. Gault, F. Danoix, K. Hoummada, D. Mangelinck, H. Leitner, Impact of directional walk on atom probe microanalysis, Ultramicroscopy 113 (2012) 182–191.
[33] D.J. Larson, P.H. Clifton, N. Tabat, A. Cerezo, A.K. Petford-Long, R.L. Martens, T.F. Kelly, Atomic-scale analysis of CoFe/Cu and CoFe/NiFe interfaces, Applied Physics Letters 77 (2000) 726–728.
[34] P. Jessner, R. Danoix, B. Hannoyer, F. Danoix, Investigations of the nitrided subsurface layers of an Fe–Cr–model alloy, Ultramicroscopy 109 (2009) 530–534.
[35] F. Danoix, G. Grancher, A. Bostel, D. Blavette, Standard deviations of composition measurements in atom probe analyses: part II 3D atom probe, Ultramicroscopy 107 (2007) 739–743.